



## On the human CYP2C9\*13 variant activity reduction: a molecular dynamics simulation and docking study

Y.-H. Zhou<sup>a</sup>, Q.-C. Zheng<sup>a</sup>, Z.-S. Li<sup>a,\*</sup>, Y. Zhang<sup>a</sup>, M. Sun<sup>a</sup>, C.-C. Sun<sup>a</sup>,  
D. Si<sup>b</sup>, L. Cai<sup>b</sup>, Y. Guo<sup>b</sup>, H. Zhou<sup>b,\*</sup>

<sup>a</sup> State Key Laboratory of Theoretical and Computational Chemistry, Institute of Theoretical Chemistry, Jilin University, Changchun 130023, China

<sup>b</sup> College of Life Science, Jilin University, Changchun 130023, China

Received 23 December 2005; accepted 1 May 2006

### Abstract

Cytochrome P450 2C9 (CYP2C9) plays a key role in the metabolism of clinical drugs. CYP2C9 is a genetically polymorphic enzyme and some of its allelic variants have less activity compared to the wild-type form. Drugs with a narrow therapeutic index may cause serious toxicity to the individuals who carry such allele. CYP2C9\*13, firstly identified by some of the present authors in a Chinese poor metabolizer of lornoxicam, is characterized by mutation encoding Leu90Pro substitution. Kinetic experiments show that CYP2C9\*13 has less catalytic activity in elimination of diclofenac and lornoxicam in vitro. In order to explore the structure–activity relationship of CYP2C9\*13, the three-dimensional structure models of the substrate-free CYP2C9\*1 and its variant CYP2C9\*13 are constructed on the basis of the X-ray crystal structure of human CYP2C9\*1 (PDB code 1R9O) by molecular dynamics simulations. The structure change caused by Leu90Pro replacement is revealed and used to explain the dramatic decrease of the enzymatic activity in clearance of the two CYP2C9 substrates: diclofenac and lornoxicam. The trans configuration of the bond between Pro90 and Asp89 in CYP2C9\*13 is firstly identified. The backbone of residues 106–108 in CYP2C9\*13 turns over and their side chains block the entrance for substrates accessing so that the entrance of \*13 shrinks greatly than that in the wild-type, which is believed to be the dominant mechanism of the catalytic activity reduction. Consequent docking study which is consistent with the results of the kinetic experiments by Guo et al. identifies the most important residues for enzyme–substrate complexes.

© 2006 Elsevier SAS. All rights reserved.

**Keywords:** Cytochrome P450 2C9; CYP2C9\*13; Genetic polymorphisms; Structure–activity; Molecular dynamics simulation

### 1. Introduction

Cytochrome P450s (CYPs) are the most important superfamily of biotransformation enzymes that are involved in oxidative metabolism of a wide variety of endogenous and exogenous compounds [1–3]. The CYP2C subfamily of human liver P450 isozymes is of major importance in drug metabolism and plays a key role in the drugs pharmacological and toxicological effects [4]. CYP2C9 is the most abundant 2C subfamily isozyme in human liver which is responsible for the metabolic clearance of a wide variety of the therapeutic agents, estimated up to 16% of drugs in current clinical used [5].

The human *CYP2C9* gene is highly polymorphic. At least 24 *CYP2C9* alleles have been identified to date and most of them show reduced activity (<http://www.imm.ki.se/CYPalleles/cyp2c9.htm>). Some narrow therapeutic index drugs, of which very small changes in the dosage level could cause toxic results, may lead more dangerous to the individuals who carries mutant *CYP2C9* allele. Numerous studies have been performed in vitro and in vivo to evaluate the influence of *CYP2C9* genotypes on metabolic activity and drug disposition [5–11]. How these different alleles influence enzymatic activity has attracted much interest.

A *CYP2C9* allele designated *CYP2C9\*13* has been identified in a Chinese poor metabolizer of lornoxicam [12]. This allele involves a T269C transversion in exon 2 that leads to a Leu90Pro substitution in the encoded protein, with an allele frequency of about 1.02% in the Chinese population [12] and

\* Corresponding authors.

E-mail addresses: [zeshengli@mail.jlu.edu.cn](mailto:zeshengli@mail.jlu.edu.cn) (Z.-S. Li), [zhouhui@mail.jlu.edu.cn](mailto:zhouhui@mail.jlu.edu.cn) (H. Zhou).

0.6% in the Korea population [13]. Two classical substrates, lornoxicam and diclofenac, were chosen to measure the catalytic activity of CYP2C9 [7,8,14]. Results of the kinetic experiments showed that CYP2C9\*13 had lower intrinsic clearance than CYP2C9\*1 due to the increase in Michaelis–Menten constant ( $K_m$ ) and decrease in maximal reaction velocity ( $V_{max}$ ) and the metabolic impact of CYP2C9\*13 depends on the substrate being metabolized (Table 1). The mutant CYP2C9 allele which has lower activity is associated with increased risk of adverse drug events. Therefore, it is of significance to find out the reasons for the decreasing activity of CYP2C9\*13 for clinic therapy.

CYP2C9 is the first human P450 isozyme that the X-ray crystal structures both unliganded and in complex with warfarin has been determined by Williams et al. [15] (PDB code 1OG2/1OG5). Then, Wester et al. [16] determined the structure of CYP2C9 complexed with flurbiprofen (PDB code 1R9O). The X-ray crystal structures can help to understand the structure–function relationship of CYP2C9, but the relationship between structure and lower catalytic activity of its natural allelic variant CYP2C9\*13 are still unclear.

Before CYP2C9 crystal structure was determined, many research groups [17–20] had used the method of homology modeling based on the X-ray crystal structure of CYP2C5 etc. to construct the three-dimensional (3D) model of CYP2C9. In this study, 3D structures of substrate-free CYP2C9\*1 and \*13 were constructed based on the X-ray crystal structure of wild-type CYP2C9 complexes with flurbiprofen (PDB code: 1R9O). They were then used to characterize the explicit enzyme complexes with two structurally and chemically diverse substrates, lornoxicam and diclofenac, in order to identify the most important residues in CYP2C9\*13 for binding the two substrates.

## 2. Methods

All molecular modeling studies were performed on SGI O3800 workstation using Gaussian 03 [21] and the InsightII software package developed by Accelrys [22]. The consistent-valence force field (CVFF) was used for energy minimization and molecular dynamics (MD) simulations.

### 2.1. MD simulations

The X-ray crystal structure of CYP2C9/flurbiprofen complex (PDB code 1R9O) [16] was used as a starting structure and was employed to construct substrate-free forms of the wild-type CYP2C9 and Leu90Pro mutants. Because the con-

figuration of the bond between Pro90 and Asp89 in the mutant was unknown, the models with trans- and cis-forms of Pro90 were both constructed. The three 3D models were named as \*1, \*13-trans and \*13-cis.

The first 22 amino acid residues in N-terminus which contained the transmembrane signal anchor domain were deleted in 1R9O and also not recruited in the 3D models as they are away from the active site. Residues 38–42 and residues 214–220 lost in the crystal structure were complemented by Loop Search in InsightII/homology module. The residue replacement was performed by using InsightII/Biopolymer module. All of the 3D models were solvated in a layer of TIP3P water molecules [23] with radius 10 Å, and their protonation states were set at physiological pH 7.5 in which the experiment performed. To refine these initial 3D models, after performing 200 steps of conjugate gradient (CG) minimization, 1 ns MD simulation without any restraints was carried out at a constant temperature 300 K. Finally, a CG energy minimization of full protein was performed until the root-mean-square (RMS) gradient energy was lower than 0.001 kcal mol<sup>-1</sup>. All the energy minimization and MD simulations mentioned above were accomplished by using Discover-3 module [24] of the InsightII software. During the optimization procedure, the structure was checked by Profile-3D [25,26] and ProStat. The Profile-3D is used in testing the validity of hypothetical protein structures by measuring the compatibility of the hypothetical structure with its own amino acid sequence. The ProStat module of InsightII is used to identify and list the number of instances where the structural features differ significantly from the average values calculated from the known proteins.

### 2.2. Flexible docking

Affinity [27], a suite of programs for automatically docking a ligand to a receptor in InsightII software package using a combination of Monte Carlo type and simulated annealing (SA) method, features for its semi-flexible method that the “bulk” of the receptor, defined as atoms not in the binding-site specified, is held rigid during the docking process. In the docking process, the potential function of the complex was assigned by using the CVFF force field and the non-bonding interaction was dealt with cell-multiple approach. To consider the solvent effect, the centered enzyme–ligand complexes were solvated in a sphere of TIP3P water molecules with radius 10 Å. All the default parameters in the Affinity module were used. It provided 10 conformations from SA docking, and the generated conformations were clustered according to the RMS deviation (RMSD). The docked complexes were finally

Table 1

Kinetic parameters for diclofenac 4'-hydroxylation and lornoxicam 5'-hydroxylation by postmitochondrial supernatant (S9) from COS-7 cells expressing wild-type and variant CYP2C9s

	Diclofenac 4'-hydroxylation		Lornoxicam 5'-hydroxylation	
	*1	*13	*1	*13
$K_m$ (μM)	2.33 ± 0.17	11.60 ± 2.56**	1.24 ± 0.09	2.79 ± 0.26**
$V_{max}$ (pmol min <sup>-1</sup> pmol <sup>-1</sup> )	27.15 ± 0.94	3.04 ± 0.24**	0.83 ± 0.02	0.22 ± 0.01**
$V_{max}/K_m$ (μl min <sup>-1</sup> pmol <sup>-1</sup> )	11.71 ± 0.56	0.29 ± 0.01**	0.68 ± 0.05	0.08 ± 0.01**

Each value represents the mean ± S.E.M. of independent experiments. \*\* $P < 0.01$  vs. CYP2C9\*1 [8,14].

selected by the criterion of the total energy combined with the geometrical matching quality and favorable interaction energy. The 3D structures of lornoxicam and diclofenac for docking study were optimized using semi-empirical method AM1 of Gaussian 03 software.

### 3. Results and discussion

#### 3.1. 3D structures of CYP2C9\*1 and \*13

Williams et al. [15] and Wester et al. [16] obtained the X-ray structure of CYP2C9 successively. In this work, 1R9O, the result of Wester et al., has been used as the initial structure in further simulations, for its better resolution and less residues has been substituted in the crystal structure. The trans/cis configuration of the bond between Asp89 and Pro90 in CYP2C9\*13 has

not been determined in experiments. In this work, besides the substrate-free 3D model of CYP2C9\*1, two 3D models of \*13 with the configurations of trans- or cis-state were constructed, respectively. The stability of these 3D models was refined by performing MD simulations. Fig. 1 displays potential energy of the simulated systems during the 1 ns of MD. As seen from Fig. 1, all the systems are structurally stable after 600 ps MD time. Of these, the conformation with the lowest energy is chosen for each system. The RMSD, the Profiles-3D and the ProStat methods were used to evaluate the built 3D models compare with the crystal structure of 1R9O and the results are listed in Table 2. No significant differences between the calculated values of the bond lengths and bond angles for the total residues compared with that of the known proteins were found by the ProStat analysis. These information indicates that these 3D models are reliable for further docking studies.

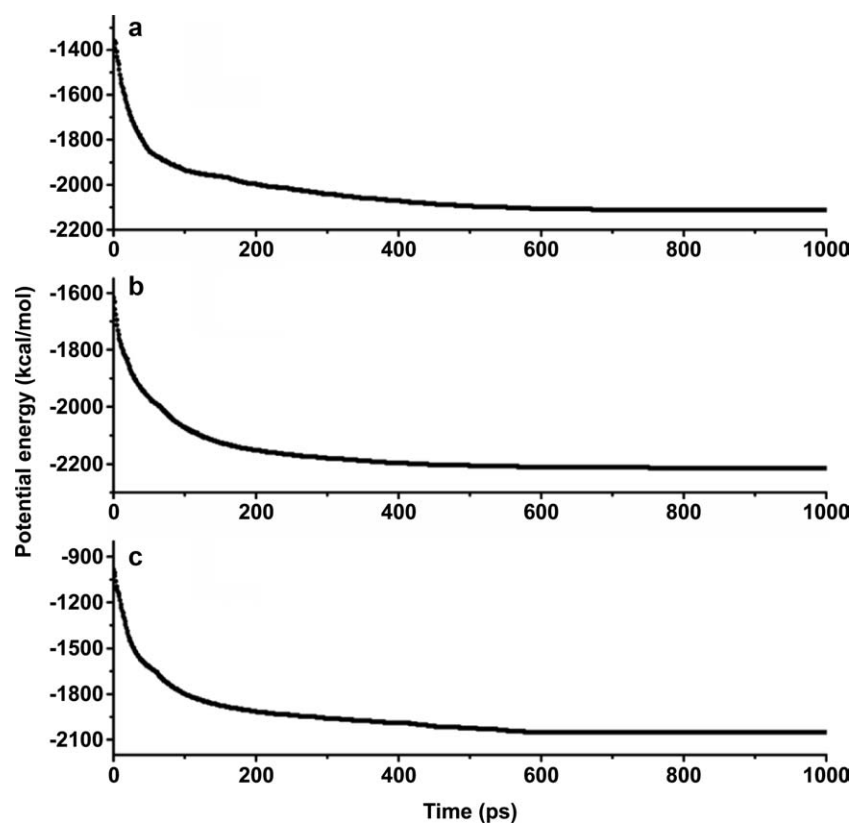


Fig. 1. The variation of the potential energy during the 1 ns of MD on (a) \*1, (b) \*13-trans, (c) \*13-cis.

Table 2  
Comparison of the \*1, \*13-trans, \*13-cis models and 1R9O X-ray structure

	1R9O/*1	*1/*13-trans	*1/*13-cis	
RMSD <sup>a</sup> (Å)	0.611	0.605	0.706	
Profile-3D scores (expected score)	200.7(207) <sup>b</sup>	209.2(212) <sup>c</sup>	212.3(212) <sup>c</sup>	209.3(212) <sup>c</sup>
ProStat (%Φ-ψ angles in core Ramachandran region)	84.2%	72.7%	76.4%	75.1%

<sup>a</sup> RMSD of Ca position.

<sup>b</sup> Expected score for 455 residues.

<sup>c</sup> Expected score for 465 residues.

InsightII/binding-site module is used to search the residues on the surface of the enzyme for substrate accessing based on the known binding-site of 1R9O. Ala106, Arg108, Leu234, Val237, Ala238, Lys241 and Val292, which map to the B–C loop, helix G and helix I, respectively, are found to compose the entrance for substrates accessing. The variations of distances between two pairs of atoms which were approximated to the two crossed diameters of the substrate entrance and used to depict the size of the entrance were monitored during the MD simulation (Fig. 2). Seen from Fig. 2(a, b), the average values of the distances were stable after 600 ps, and the two distances in (a) and (b) in \*1 were larger than those in \*13-trans and \*13-cis, and the distances of (a) and (b) in \*13-cis were the smallest. Fig. 3(a–c) shows the shape and the hydrophobic quality of the entrance for substrate accessing on the surface of the enzymes. It is obvious that the substrate entrance of \*1 is the largest one in the three 3D models, followed by \*13-trans and \*13-cis models with tremendous change. In \*13-cis, even there is no entry can be found extended from the active site cavity. It is believed that the wild-type CYP2C9 has high activity as the substrates can easily go through the entrance and interact with the heme directly and rapidly on a certain degree, and such an enzyme like \*13-cis without entrance for substrates accessing can not have activity. Although CYP2C9\*13 has lower efficiency in eliminating diclofenac and lomoxicam compared to CYP2C9\*1, it still have enzymic activity, seen from Table 1. At the same time, the Asp-Pro configuration in all the deposited structure of P450 enzymes in Protein Data Bank (<http://www.rcsb.org/pdb/>) have been explored, and all of them are trans state. Thus, the configuration of Pro90 bond with Asp89 in \*13 is identified as trans state and only \*1 and \*13-trans 3D models are selected for further analysis and docking studies. The term, \*13-trans, are replaced by \*13 for shorten in the following discussions.

Leu90 in the wild-type CYP2C9 is at the head of the B–C loop. An overlap of  $C\alpha$  of the \*1 and \*13 models (Fig. 4) shows that a long-range effect occurs on the B–C loop when Leu is replaced by Pro. The backbones of Residues 106–108 turn over and the side chains of Ala106 and Arg108 block

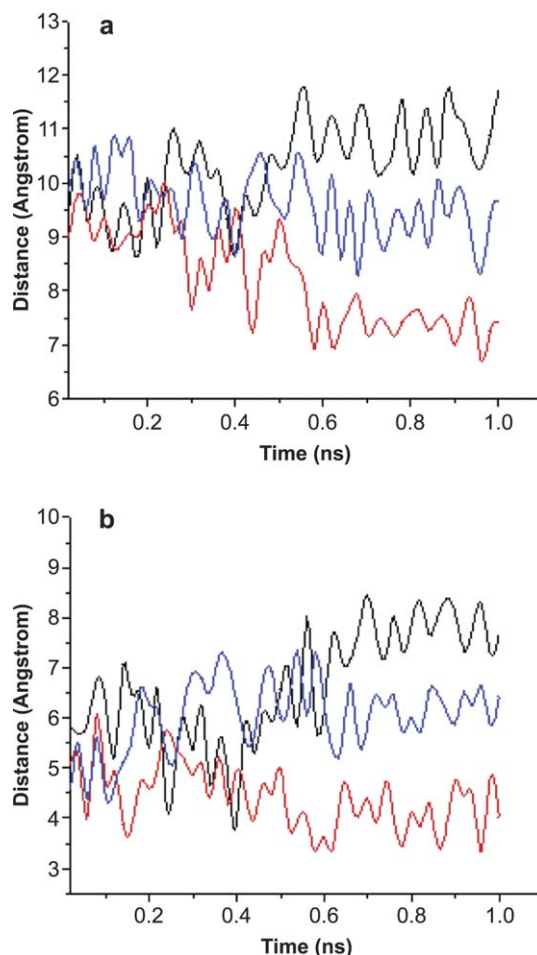


Fig. 2. Variation of distances between (a) terminal C of Arg108 and  $C\alpha$  of Val292; (b)  $C\beta$  of Ala106 and  $C\alpha$  of Leu234 during the 1 ns MD simulation. \*1 represented by black, \*13-trans represented by blue and \*13-cis represented by red.

parts of entrances. It is known that the active site of CYP2C9 enzyme is buried and the enzyme must undergo a conformational change in order for the lipophilic substrate to go through a long channel to reach the active site. The characters of the entrance surface, such as the shape, the size or the static poten-

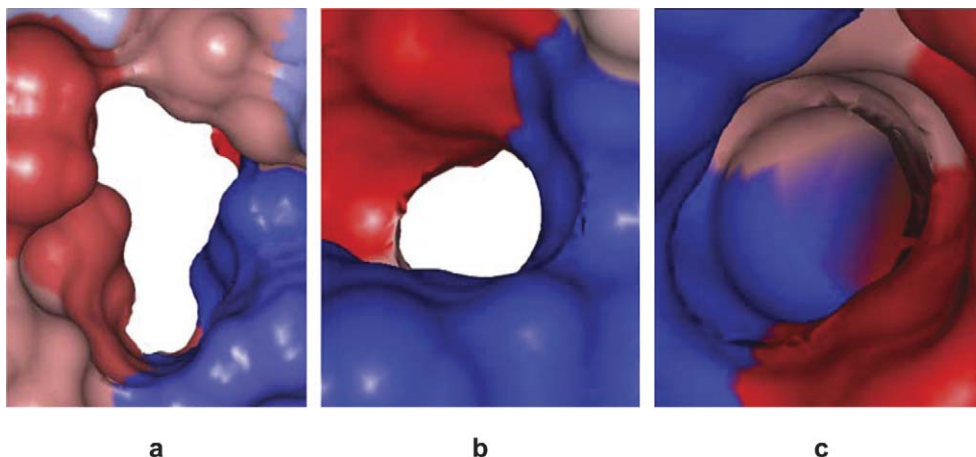


Fig. 3. The solvent accessible surfaces of the entrance for substrate accessing on the enzymes' surface of the three models (a) \*1, (b) \*13-trans, (c) \*13-cis, hydrophilic residues represented by blue color, hydrophobic residues represented by red color.

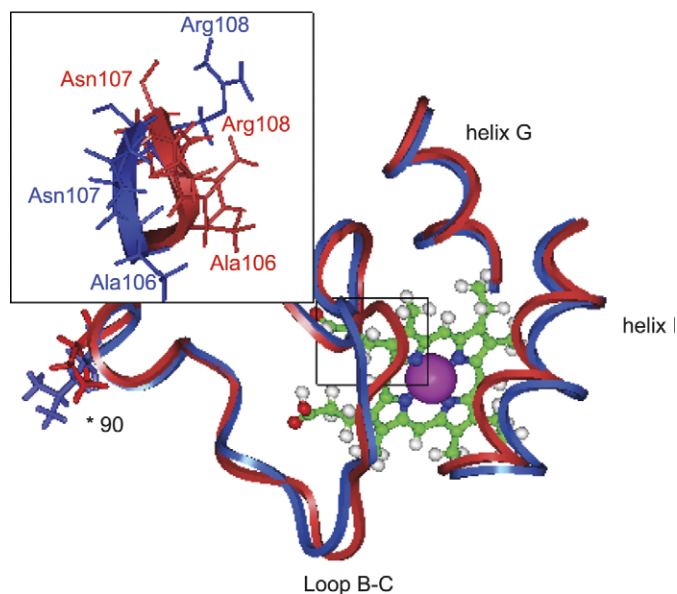


Fig. 4. The overlap of Ca of the \*1 and \*13-trans models. \*1 model is represented by blue color, \*13-trans model is represented by red color.

tial etc., are important factors for the enzymatic activity of CYP, which have been investigated by several research groups [28–30]. For \*13, hydrophilic residue Arg108 exposes completely on the surface of the enzyme, so that the hydrophobic state of the surface near the entrance is weakened to some extent. The possible reason of the catalytic activity reduction is the lipophilic substrates can not be closed to the entrance easily. The size of the entrance shrinks largely and the shape also changes (Fig. 3(a, b)). The processes of the substrate accessing to the active site and the product releasing from the active site may be retarded depending on the different size of the molecules due to the smaller entrance. The size of the substrate entrance may be one of the influencing factors for the catalytic activity of an enzyme. Owing to the presence of chlorine substituents and the staggered conformation of the two aromatic rings [31], diclofenac and its product, 4'-OH-diclofenac, may encounter more sterically block during the catalytic process compared to lornoxicam. This is in accordance with the results of the kinetic experiments (Table 1) that the metabolism of diclofenac by CYP2C9\*13 decreases remarkably than that of lornoxicam.

### 3.2. Docking study

The CYP2C9 substrates have the typically common features such as hydrophobic regions, aromatic groups, hydrogen bond accepting sites and hydrogen bond donating sites for some substrates. The substrates have therefore been suggested to interact with the enzyme via hydrogen bonding, ion-pair to charged amino acids and  $\pi$ - $\pi$  stacking with aromatic residues in the active site [1,18,32].

The two substrates have the common hydrophobic head and hydrogen bond accepting sites as presented in Fig. 5, while diclofenac is an acidic compound and mainly exists as anions at physiological pH and is apt to bind with CYP2C9\*1 as anions whereas lornoxicam is in neutral forms [31,33]. In addi-

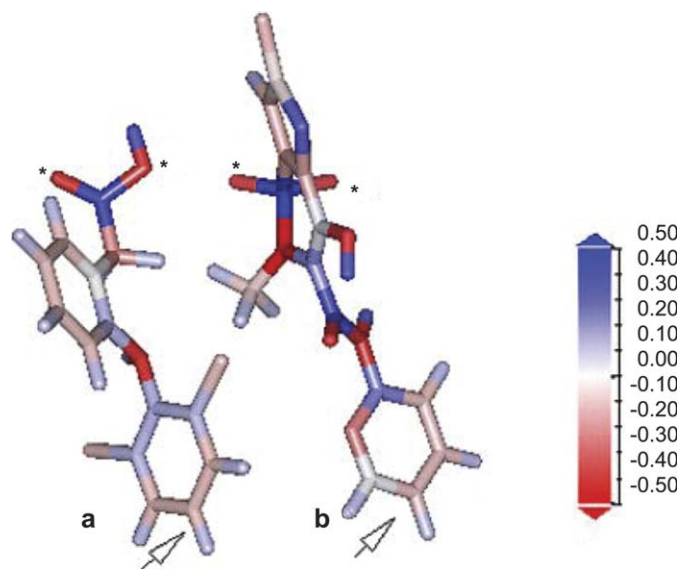


Fig. 5. The structures of the (a) diclofenac, (b) lornoxicam optimized by AM1 method, colored by surface static potential. Arrows point to the site which can be hydroxylated by the enzyme and asterisk signed the possible H-bond acceptors (all of them are oxygens).

tion, diclofenac also has a phenyl which can interact with the aromatic residues of the enzyme by  $\pi$ - $\pi$  stacking. Lornoxicam and diclofenac, two kinds of non-steroidal anti-inflammatory drugs (NSAIDs), are primarily metabolized by CYP2C9 to 5'-hydroxylornoxicam [34] and 4'-hydroxydiclofenac [35], respectively. The kinetic experiments of metabolism of diclofenac and lornoxicam by CYP2C9\*13 showed that the decrease of the intrinsic clearance was depending on the substrate. In order to understand the catalytic mechanism, a flexible docking study is carried out to reveal the interaction between the different substrates and enzymes.

#### 3.2.1. Docking of the diclofenac into the active site

The diclofenac-\*1, diclofenac-\*13 complexes are generated using the InsightII/Affinity module. The superposition of the binding 3D conformation within the active site of the diclofenac-\*1 and diclofenac-\*13 complexes are shown in Fig. 6. Diclofenac is stabilized by hydrogen bonding and hydrophobic interactions in the center of the active site. The hydrogen bonds presented in the complexes are listed in Table 3. In diclofenac-\*1 complex, two oxygens in the carboxyl group of diclofenac are hydrogen bonded to Arg108 and Asn204, respectively. Three H-bonds are formed, two with Arg108 and one with Asn204. In diclofenac-\*13 complex, only two H-bonds are formed, one is between the one of the oxygens in carbonyl group of diclofenac and Arg108, the other one is formed between the other oxygen in carbonyl of diclofenac and Asn204. The hydrogen bonding interactions stabilize the complex so that less H-bonds lead to less stable for diclofenac in CYP2C9\*13 active site. The orientation of diclofenac in the active site altered for less H-bonds and the distance from the 4'-carbon atom which can be hydroxylated to the heme in \*13 (4.54 Å) is a little longer than that in \*1 (4.21 Å). Both distances are fit for forming the 4'-hydroxylated product, but the

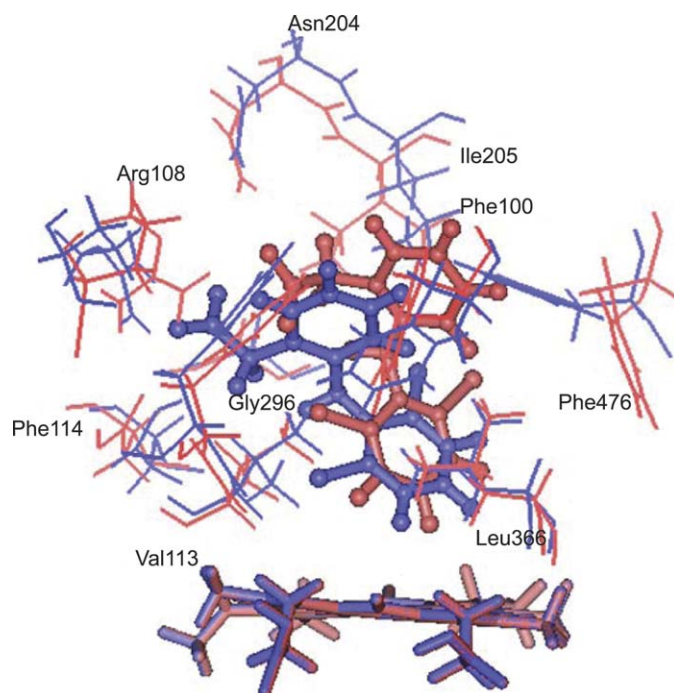


Fig. 6. An overlap of docking results of diclofenac. Diclofenac-\*1 complex represented by blue color, diclofenac-\*13 complex represented by red color. Diclofenac is rendered as ball and stick, heme is rendered as stick.

efficiency of eliminating diclofenac with \*13 may be affected due to the decrease of the interaction energy between heme and diclofenac caused by the longer distance.

To find the key residues in the complexes, the interaction energies of the ligand with each of the residues in the active site for both complexes are calculated. Significant binding-site residues in the 3D models are identified by the total interaction energy between the ligand and each amino acid residues in each enzyme. In general, if the interaction energy between the residues and the substrate is lower than  $-1 \text{ kcal mol}^{-1}$ , those residues are considered to be important in the substrate binding complex. In diclofenac-\*1 or diclofenac-\*13 complexes, so many residues have stronger attractive energy with diclofenac and the residues which have the interaction energy lower than  $-4 \text{ kcal mol}^{-1}$  are considered to be more important. The interaction energies including the total, van-der-Waals and electrostatic energies of those residues in the diclofenac-\*1 and diclofenac-\*13 complexes are shown in Table 4(a, b). The diclofenac-\*1 complex has a large favorable total interaction energy of  $-125.91 \text{ kcal mol}^{-1}$ , the van-der-Waals and electrostatic energies are  $-46.25$  and  $-79.66 \text{ kcal mol}^{-1}$ , respectively.

Table 3

The angle and distance of H-bond formed in docking of diclofenac, and the distance between the oxidation site of the substrate and Fe of heme

	Donors	Acceptors	Distance (Å)	Angle (°)	Distance <sub>Fe-C</sub> (Å)
*1	Arg108	Carboxyl O1	2.27	142.43	4.21
	Arg108	Carboxyl O1	1.71	169.71	
	Asn204	Carboxyl O2	1.74	154.26	
*13	Arg108	Carboxyl O1	1.95	160.86	4.54
	Asn204	Carboxyl O1	2.27	134.16	

Table 4

The total energy ( $E_{\text{total}}$ ), van-der-Waals energy ( $E_{\text{vdw}}$ ) and electrostatic energy ( $E_{\text{ele}}$ ) between diclofenac and individual residues in CYP2C9\*1 (a) and CYP2C9\*13 (b) (contain heme) ( $E_{\text{total}} < -4.00 \text{ kcal mol}^{-1}$  listed in energy rank order)

Residue	$E_{\text{vdw}}$ (kcal mol <sup>-1</sup> )	$E_{\text{ele}}$ (kcal mol <sup>-1</sup> )	$E_{\text{total}}$ (kcal mol <sup>-1</sup> )
a			
Total	-46.25	-79.66	-125.91
Asp293	0.35	-31.63	-31.28
Arg108	0.82	-18.02	-17.20
heme	-10.20	-4.35	-14.55
Val113	-4.06	-6.12	-10.18
Gly296	-2.18	-5.02	-7.20
Leu366	-4.94	-1.14	-6.08
Phe476	-3.47	-1.38	-4.85
Phe114	-3.16	-1.41	-4.57
Asn204	-0.53	-4.00	-4.53
Phe100	-3.27	-0.91	-4.18
Ile205	-3.11	-1.03	-4.14
b			
Total	-51.59	-22.24	-73.83
heme	-8.22	-1.84	-10.06
Asn204	-1.62	-7.80	-9.42
Gly296	-2.31	-4.66	-6.97
Leu208	-3.27	-3.37	-6.64
Phe100	-4.28	-2.19	-6.47
Phe114	-2.24	-3.69	-5.93
Val113	-1.11	-4.31	-5.42
Leu366	-3.49	-1.41	-4.90
Ile205	-4.68	-0.15	-4.83
Arg108	-0.76	-3.65	-4.41

And the diclofenac-\*13 complex has a favorable total interaction energy of  $-73.83 \text{ kcal mol}^{-1}$ , the van-der-Waals and electrostatic energies are  $-51.59$  and  $-22.24 \text{ kcal mol}^{-1}$ , respectively. These results indicate that the decrease of the electrostatic attractive energy is the main reason that the total attraction energy is weaker in \*13 than in \*1. The smaller attractive energy means the less affinity between the substrate and enzyme. In general, smaller the apparent  $K_m$ , the greater the affinity an enzyme has for its substrate. Compared with the wild-type, the apparent  $K_m$  value of CYP2C9\*13 for diclofenac is increased fivefold (Table 1), and in our docking result the total attractive energy decrease 41% which is in harmony with the kinetic experiment by Guo et al. [7,14] well.

The attractive interaction of electrostatic or van-der-Waals between heme and the substrate are both important for the substrate binding orientation and the attractive interaction is absolutely necessary for the hydroxylation mechanism [36]. Through interaction energy analysis, it is found that both in diclofenac-\*1 and diclofenac-\*13 complexes, some residues such as Phe100, Val113, Phe114, Asn204, Ile205, Gly296, and Leu366 are the most important anchoring residues for binding with diclofenac. Although Asp293 in CYP2C9\*1 has a sizable electrostatic attractive with the diclofenac, there is almost no such interaction in diclofenac-\*13 complex. This may be the reason that the attractive energy decreases so much for diclofenac-\*13. The study of Asp293 site-mutations by Flanagan et al. [37] indicates that the carboxyl group of the Asp293 has interaction with the substrate diclofenac, and the

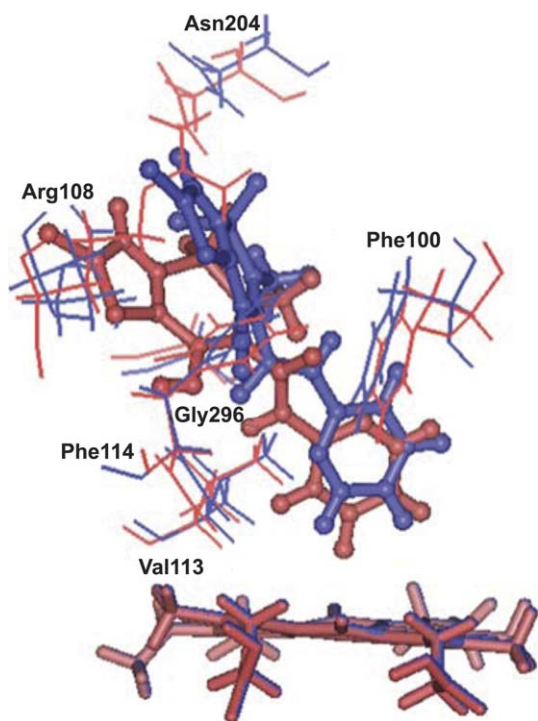


Fig. 7. An overlap of docking results of lornoxicam. Lornoxicam-\*1 complex represented by blue color, lornoxicam-\*13 complex represented by red color. Lornoxicam is rendered as ball and stick, heme is rendered as stick.

replacement of Asp293 with Ala leads to 10-fold increase in  $K_m$  values for diclofenac. Arg108 is also found important as it can form H-bond with diclofenac in diclofenac-\*1 complex and this result is identical with that in the report of Ridderstrom et al. [38]: the mutation of Arg108 makes the enzyme inactive in eliminating diclofenac compared to the wild-type enzyme. Melet et al. [39] indicated that Phe476 in CYP2C9 is an important residue for the substrate selectivity and it can have  $\pi$ - $\pi$  stacking interaction with substrates. Phe476 in \*1 is found necessary for binding diclofenac for the sizable attractive energy in the diclofenac-\*1 complex. However, in diclofenac-\*13 complex, the attractive interaction energy between diclofenac and Arg108, Phe476, respectively, weaken greatly. As shown in Table 4, Phe476 of \*13 has no  $\pi$ - $\pi$  stacking interaction with diclofenac owing to the small  $E_{ele}$  (the data does not list in Table 4(b) for the energy more than  $-4$  kcal mol $^{-1}$ ). The changes above are considered to significantly decrease the affinity of diclofenac-\*13 complex.

### 3.2.2. Docking of the lornoxicam into the active site

The binding 3D conformations of lornoxicam-\*1, lornoxicam-\*13 complexes are shown in Fig. 7. The hydrogen bonds

Table 5

The angle and distance of H-bond formed in docking of lornoxicam, and the distance between the oxidation site of the substrate and Fe of heme

	Donors	Acceptors	Distance (Å)	Angle (°)	Distance <sub>Fe-C</sub> (Å)
*1	Arg108	Sulfone O1	2.16	157.46	4.75
	Asn204	Sulfone O2	2.06	143.82	
*13	Asn204	Sulfone O1	1.83	161.96	4.93

present in the complex are listed in Table 5. In the two complexes, lornoxicam locates in the center of the active site, and there are two H-bonds formed between lornoxicam and \*1, but one between lornoxicam and CYP2C9\*13. Like diclofenac, less H-bond reduce the stability of the lornoxicam-\*13 complex. Also, the distance from the hydroxylated site of lornoxicam to the heme in \*13 (4.93 Å) is a little longer than that in \*1 (4.75 Å). The attractive interaction energy between lornoxicam and heme in \*13 is less than that in \*1 either. These information indicate that the lornoxicam-\*1 complex has better affinity than the lornoxicam-\*13 complex.

The interaction energies of the lornoxicam with each residue in the active site of both \*1 and \*13 are calculated. We consider that the residues which have interaction energy with lornoxicam lower than  $-3$  kcal mol $^{-1}$  are the most important in the binding complex. The interaction energies including the total, van-der-Waals and electrostatic energies in the lornoxicam-\*1 and lornoxicam-\*13 complexes are shown in Table 6 (a, b). These results indicate that the van-der-Waals interaction is more important than electrostatic energies for both complexes. Compared with diclofenac, the electrostatic interaction is much smaller in lornoxicam-enzyme complex because lornoxicam is in neutral form while diclofenac has net charge at physiological pH 7.5. Compared with the wild-type, the apparent  $K_m$  value of CYP2C9\*13 for lornoxicam increased 2.3-fold. Our docking results show that the total interaction energy decreases 20%. As is well known, the larger apparent  $K_m$  value the substrate has, the smaller affinity between substrate and enzyme is and the attractive energy between substrate and enzyme can express approximately to their affinity. Thus, both results of the diclofenac and lornoxicam are in harmony with this fact.

Table 6

The total energy ( $E_{total}$ ), van-der-Waals energy ( $E_{vdw}$ ) and electrostatic energy ( $E_{ele}$ ) between lornoxicam and individual residues in CYP2C9\*1 (contain heme) ( $E_{total} < -3.00$  kcal mol $^{-1}$  listed in energy rank order)

Residue	$E_{vdw}$ (kcal mol $^{-1}$ )	$E_{ele}$ (kcal mol $^{-1}$ )	$E_{total}$ (kcal mol $^{-1}$ )
a			
Total	-62.29	-8.24	-70.53
heme	-10.00	-1.85	-11.85
Arg108	-6.46	-1.17	-7.63
Val113	-3.89	-0.42	-4.31
Gly296	-2.95	-1.35	-4.30
Phe100	-4.72	0.47	-4.25
Ala297	-3.25	0.83	-4.08
Phe114	-3.48	-0.56	-4.04
Asn204	-1.74	-2.20	-3.94
Ile205	-3.94	0.77	-3.17
b			
Total	-54.65	-1.90	-56.55
heme	-7.01	-1.51	-8.52
Gly296	-4.30	-0.30	-4.60
Phe114	-4.94	1.01	-3.93
Asp293	-3.62	-0.07	-3.69
Leu366	-2.93	-0.40	-3.33
Phe100	-2.31	-0.86	-3.17
Val113	-4.08	0.96	-3.12
Asn204	-1.28	-1.74	-3.02

The interaction energy between heme and lornoxicam is dominant whether in lornoxicam-\*1 complex or in lornoxicam-\*13 complex. In both complexes, the most important anchoring residues for binding with lornoxicam are Phe100, Val113, Phe114, Asn204 and Gly296. Lornoxicam has little interaction with Arg108 in \*13 and Asn204 becomes more important in CYP2C9\*13 substrate selectivity, like diclofenac.

#### 4. Conclusion

CYP2C9 polymorphisms are associated with increasing the risk of adverse drug events and arouse an extensive research. A mutant allele, CYP2C9\*13, which has a Leu90Pro amino acid substitution has been identified by some of the present authors [12]. Consequent kinetic study in vitro indicates that this variant of CYP2C9 has less active in eliminating diclofenac and lornoxicam by the increase of  $K_m$  and the decrease of  $V_{max}$  depending on the substrate. For investigating the mechanism of the catalytic activity reduction, in this study, 3D models of substrate-free CYP2C9\*1 and CYP2C9\*13 variant are constructed based on the crystal structure 1R9O and optimized by MD simulation. Assessed by Profile-3D and ProStat, the final 3D models are reliable. For the first time, trans configuration of the bond between Pro90 and Asp89 in CYP2C9\*13 was identified. Furthermore, by comparing the \*1 and \*13-trans models, a long-range effect on the residues 106–108 which are part of the entrance constitution caused by the Leu90Pro substitution was found. The backbone of 106–108 turns over and their side chains block the entry which may be the dominant mechanism of the catalytic activity reduction of CYP2C9\*13. After the docking study, the most important residues of the CYP2C9\*1 and \*13 for binding diclofenac and lornoxicam were identified, respectively. The attractive energy which reflects the affinity of enzyme–substrate complex is consistent with the kinetic experiments well. Our results may be helpful for revealing the catalytic mechanism and further experimental studies for this kind of enzymes.

#### Acknowledgments

This work was supported by the National Science Foundation of China (20333050, 20073014, 30472062), Doctor Foundation by the Ministry of Education, Foundation for University Key Teacher by the Ministry of Education, Key Subject of Science and Technology by the Ministry of Education of China, and Key Subject of Science and Technology by Jilin Province.

#### References

- [1] I.G. Denisov, T.M. Makris, S.G. Sligar, I. Schlichting, Structure and chemistry of cytochrome P450, *Chem. Rev.* 105 (2005) 2253–2277.
- [2] F.P. Guengerich, Common and uncommon cytochrome P450 reactions related to metabolism and chemical toxicity, *Chem. Res. Toxicol.* 14 (2001) 611–650.
- [3] D.W. Nebert, F.J. Gonzalez, P450 genes: structure, evolution, and regulation, *Annu. Rev. Biochem.* 56 (1987) 945–993.
- [4] J.A. Goldstein, S.M.F. Demorais, Biochemistry and molecular-biology of the human Cyp2C subfamily, *Pharmacogenetics* 4 (1994) 285–299.
- [5] U.I. Schwarz, Clinical relevance of genetic polymorphisms in the human CYP2C9 gene, *Eur. J. Clin. Invest.* 33 (2003) 23–30.
- [6] U. Yasar, E. Eliasson, C. Forslund-Bergengren, G. Tybring, M. Gadd, F. Sjoqvist, M.L. Dahl, The role of CYP2C9 genotype in the metabolism of diclofenac in vivo and in vitro, *Eur. J. Clin. Pharmacol.* 57 (2001) 729–735.
- [7] Y.J. Guo, Y.F. Zhang, Y. Wang, X.Y. Chen, D.Y. Si, D.F. Zhong, J.P. Fawcett, H. Zhou, Role of CYP2C9 and its variants (CYP2C9\*3 and CYP2C9\*13) in the metabolism of lornoxicam in humans, *Drug Metab. Dispos.* 33 (2005) 749–753.
- [8] Y.F. Zhang, D.F. Zhong, D.Y. Si, Y.J. Guo, X.Y. Chen, H. Zhou, Lornoxicam pharmacokinetics in relation to cytochrome P4502C9 genotype, *Br. J. Clin. Pharmacol.* 59 (2005) 14–17.
- [9] J. Shimamoto, I. Ieiri, A. Urae, M. Kimura, S. Irie, T. Kubota, K. Chiba, T. Ishizaki, K. Otsubo, S. Higuchi, Lack of differences in diclofenac (a substrate for CYP2C9) pharmacokinetics in healthy volunteers with respect to the single CYP2C9\*3 allele, *Eur. J. Clin. Pharmacol.* 56 (2000) 65–68.
- [10] K. Takamashi, H. Tainaka, K. Kobayashi, T. Yasumori, M. Hosakawa, K. Chiba, CYP2C9 Ile(359) and Leu(359) variants: enzyme kinetic study with seven substrates, *Pharmacogenetics* 10 (2000) 95–104.
- [11] H. Yamazaki, K. Inoue, K. Chiba, N. Ozawa, T. Kawai, Y. Suzuki, J.A. Goldstein, F.P. Guengerich, T. Shimada, Comparative studies on the catalytic roles of cytochrome P450 2C9 and its Cys- and Leu-variants in the oxidation of Warfarin, flurbiprofen, and diclofenac by human liver microsomes, *Biochem. Pharmacol.* 56 (1998) 243–251.
- [12] D.Y. Si, Y.J. Guo, Y.F. Zhang, L. Yang, H. Zhou, D.F. Zhong, Identification of a novel variant CYP2C9 allele in Chinese, *Pharmacogenetics* 14 (2004) 465–469.
- [13] J.W. Bae, H.K. Kim, J.H. Kim, S.I. Yang, M.J. Kim, C.G. Jang, Y.S. Park, S.Y. Lee, Allele and genotype frequencies of CYP2C9 in a Korean population, *Br. J. Clin. Pharmacol.* 60 (2005) 418–422.
- [14] Y.J. Guo, Y. Wang, D.Y. Si, J.P. Fawcett, D.F. Zhong, H. Zhou, Catalytic activities of human cytochrome P450 2C9.1, 2C9.3 and 2C9.13, *Xenobiotica* 35 (2005) 953–961.
- [15] P.A. Williams, J. Cosme, A. Ward, H.C. Angova, D.M. Vinkovic, H. Jhoti, Crystal structure of human cytochrome P4502C9 with bound warfarin, *Nature* 424 (2003) 464–468.
- [16] M.R. Wester, J.K. Yano, G.A. Schoch, C. Yang, K.J. Griffin, C.D. Stout, E.F. Johnson, The structure of human cytochrome P4502C9 complexed with flurbiprofen at 2.0-angstrom resolution, *J. Biol. Chem.* 279 (2004) 35630–35637.
- [17] T. Tanaka, N. Kamiguchi, T. Okuda, Y. Yamamoto, Characterization of the CYP2C8 active site by homology modeling, *Chem. Pharm. Bull. (Tokyo)* 52 (2004) 836–841.
- [18] M.J. de Groot, A.A. Alex, B.C. Jones, Development of a combined protein and pharmacophore model for cytochrome P4502C9, *J. Med. Chem.* 45 (2002) 1983–1993.
- [19] M. Ridderstrom, I. Zamora, O. Fjellstrom, T.B. Andersson, Analysis of selective regions in the active sites of human cytochromes P450, 2C8, 2C9, 2C18, and 2C19 homology models using GRID/CPCA, *J. Med. Chem.* 44 (2001) 4072–4081.
- [20] V.A. Payne, Y.T. Chang, G.H. Loew, Homology modeling and substrate binding study of human CYP2C9 enzyme, *Proteins-Structure Function and Genetics* 37 (1999) 176–190.
- [21] M.J. Frisch, G.W. Trucks, H.B. Schlegel, Gaussian 03 (Revision A.1). *Gaussian, Pittsburgh* (2003).
- [22] InsightII Version 98.0 MSI, San Diego, USA. In 1998.
- [23] W.L. Jorgensen, J. Chandrasekhar, J.D. Madura, R.W. Impey, M.L. Klein, Comparison of simple potential functions for simulating liquid water, *J. Chem. Phys.* 79 (1983) 926–935.
- [24] Discover3 User Guide, Accelrys Inc., San Diego, 1999.

- [25] R. Luthy, J.U. Bowie, D. Eisenberg, Assessment of protein models with three-dimensional profiles, *Nature* 356 (1992) 83–85.
- [26] Profile-3D User Guide, Accelrys Inc., San Diego, 1999.
- [27] Affinity User Guide, Accelrys Inc., San Diego, 1999.
- [28] P.J. Winn, S.K. Ludemann, R. Gauges, V. Lounnas, R.C. Wade, Comparison of the dynamics of substrate access channels in three cytochrome P450s reveals different opening mechanisms and a novel functional role for a buried arginine, *Proc. Natl. Acad. Sci. USA* 99 (2002) 5361–5366.
- [29] E. Deprez, N.C. Gerber, C. Diprimo, P. Douzou, S.G. Sligar, G.H.B. Hoa, Electrostatic control of the substrate access channel in cytochrome P-450(Cam), *Biochemistry* 33 (1994) 14464–14468.
- [30] S.K. Ludemann, R.R. Gabdouliline, V. Lounnas, R.C. Wade, Substrate access to cytochrome P450cam investigated by molecular dynamics simulations: an interactive look at the underlying mechanisms, *Internet. J. Chem.* 4 (2001) (Art. No. 6).
- [31] M.R. Wester, E.F. Johnson, C. Marques-Soares, S. Dijols, P.M. Dansette, D. Mansuy, C.D. Stout, Structure of mammalian cytochrome P450 2C5 complexed with diclofenac at 2.1 Å resolution: evidence for an induced fit model of substrate binding, *Biochemistry* 42 (2003) 9335–9345.
- [32] M.J. de Groot, S.B. Kirton, M.J. Sutcliffe, In silico methods for predicting ligand binding determinants of cytochromes P450, *Curr. Top. Med. Chem.* 4 (2004) 1803–1824.
- [33] A. Mancy, P. Broto, S. Dijols, P.M. Dansette, D. Mansuy, The substrate binding site of human liver cytochrome P450 2C9: an approach using designed tienilic acid derivatives and molecular modeling, *Biochemistry* 34 (1995) 10365–10375.
- [34] P. Bonnabry, T. Leemann, P. Dayer, Role of human liver microsomal CYP2C9 in the biotransformation of lornoxicam, *Eur. J. Clin. Pharmacol.* 49 (1996) 305–308.
- [35] T. Leemann, C. Transon, P. Dayer, Cytochrome P450TB (CYP2C): a major monooxygenase catalyzing diclofenac 4'-hydroxylation in human liver, *Life Sci.* 52 (1993) 29–34.
- [36] S. Shaik, D. Kumar, S.P. de Visser, A. Altun, W. Thiel, Theoretical perspective on the structure and mechanism of cytochrome P450 enzymes, *Chem. Rev.* 105 (2005) 2279–2328.
- [37] J.U. Flanagan, L.A. McLaughlin, M.J. Paine, M.J. Sutcliffe, G.C. Roberts, C.R. Wolf, Role of conserved Asp293 of cytochrome P450 2C9 in substrate recognition and catalytic activity, *Biochem. J.* 370 (2003) 921–926.
- [38] M. Ridderstrom, C. Masimirembwa, S. Trump-Kallmeyer, M. Ahlefeldt, C. Otter, T.B. Anderson, Arginines 97 and 108 in CYP2C9 are important determinants of the catalytic function, *Biochem. Biophys. Res. Commun.* 270 (2000) 983–987.
- [39] A. Melet, N. Assrir, P. Jean, M. Pilar Lopez-Garcia, C. Marques-Soares, M. Jaouen, P.M. Dansette, M.A. Sari, D. Mansuy, Substrate selectivity of human cytochrome P450 2C9: importance of residues 476, 365, and 114 in recognition of diclofenac and sulfaphenazole and in mechanism-based inactivation by tienilic acid, *Arch. Biochem. Biophys.* 409 (2003) 80–91.